Geophysical measurements of ~~perennial snow patches~~ the Southernmost microglacier in Europe suggest permafrost occurrence in ~~Pirin Mountain,~~ Bulgaria

Gergana Georgieva[1], Christian Tzankov[2], and Atanas Kisyov[2]

[1]Sofia University "Sv. Kliment Ohridski", Sofia, Bulgaria
[2]University of Mining and Geology "Sv. Ivan Rilski", Sofia, Bulgaria

Correspondence: Atanas Kisyov (at.kisyov@gmail.com)

Abstract. Perennial snow patches are considered as indicators of permafrost ~~occurence~~occurrence. There are no large glaciers on the territory of Bulgaria but small patches of snow and firn have been observed in the high mountains at the end of the summer. In this paper we present results from the first detailed geophysical investigations of Snezhnika ~~microglacier~~glaciarret, considered as the southernmost microglacier in Europe. ~~It is~~, situated in the Golyam Kazan cirque, Pirin Mountain, Bulgaria. Ground penetrating radar (GPR) and 2D ~~Electro~~ Electrical Resistivity Tomography (ERT) were used to estimate the thickness of the ~~perennial snow patch~~ microglacier as well as its subsurface structure. Measurements started in 2018 and continued over the next ~~three~~ two years in order to ~~evaluate changes in the snow patches'~~ assess changes in its size and thickness. The mean thickness of Snezhnika is about $4-6\ m$, reaching ~~up to~~ $8\ m$ or probably higher in some areas. ERT measurements of the deeper parts of the microglacier beds show high electrical resistivities reaching over $60000\ \Omega m$ at a depth of $4-10\ m$. An anomaly at this depth is likewise distinguishable on the GPR profiles. These anomalies are interpreted as ~~frozen zones~~ permafrost areas and are consistently observed on the ERT and GPR profiles in the next two years of the study. These results imply for the first time the existence of permafrost in Pirin mountain and respectively in Bulgaria.

1 Introduction

Perennial snow patches are defined as snow fields existing for at least two consecutive summers (Watanabe, 1988). 82% of the glaciers are smaller than $0.5\ km^2$ and cover 21% of the Earth's total glaciated area (Zemp, 2006). Despite their small size, perennial snow patches and microglaciers are an important object of study for their vital role as water reservoirs for many downstream ecosystems (Milner et al., 2009; Barry et al., 2011). They are sensitive to climate change although they are less influenced by global changes than glaciers (Glazirin et al., 2004; Williams et al., 2022). Perennial snow patches survive as a result of ~~avalanching,~~ stabilization processes of accumulation as avalanching and wind-drift snow ~~and shading (Grunewald et al., 2010)~~ (Grunewald et al., 2010) and ablation (solar radiation, shading, debris) (Glazirin et al., 2004). Together with microglaciers they are important also for estimating local permafrost areas in high mountains ~~as permafrost is the last stage of the glacial life cycle~~ (Hughes, 2014, 2018).

There are no large glaciers on the territory of Bulgaria since the ~~end of the Little Ice Age~~Holocene (Gachev, 2020), but small patches of snow and firn have been observed in the high parts of the Rila and Pirin Mountains in the end of the summer. ~~Most well~~The most studied perennial snow patch in Bulgaria is Snezhnika (Gruenewald and Scheithauer, 2008; Gachev et al., 2016). It is called also "glaciarret" or microglacier due to observed moraines, indicating movements of the ice mass (Gachev, 2016). It is the modern remains of the Vihren glacier in the Pirin Mountain, varying in size between $0.02\ km^2$ and $0.07\ km^2$ (Gachev, 2017a). The first measurements of its size ~~are~~were made in the 1960's (Popov, 1964); systematic measurements ~~are~~of the size were conducted every year ~~in~~at the end of summer since 1994 (Gruenewald et al., 2008; Gachev, 2016). The size of the microglacier is well monitored but information about its thickness is sparse. In October 1957, Popov (1962) bores into the middle part of Snezhnika and reaches ground at $8\ m$. He also estimates the structure as follows: the upper $80-100\ cm$ represent an icy layer or icy crust which is under direct influence of the surface temperatures. Beneath this layer is firn consisting of grain sizes between 1 and $2\ cm$, increasing with depth. In the end of summer 2006, depth measurements were carried out again and three boreholes were made. The depth in two of them was estimated to be $11\ m$ (Gruenewald et al., 2008). Geophysical measurements for estimation of thickness and structure of microglacier were not carried out until 2018 ~~(Georgieva et al., 2019)~~(Georgieva et al., 2019; Onaca et al., 2022).

Permafrost is a section of the subsurface in which the temperature is continually below $0°$C for at least two years (Harris et al., 1988; Washburn, 1979). The definition is based exclusively on the temperature regime, and thus permafrost can exist in any type of sediment or rock (Ingeman-Nielsen, 2005). ~~Permafrost is also~~Mountain permafrost is also a good indicator for climate change ~~(Fort, 2015). The highest amplitude of temperature increase will first be visible in high mountains~~(Fort, 2015; Guodong et al., 1992). The increase of air temperature is well visible in the high mountains (Haberkorn et al., 2021). Therefore, mountain slopes with permafrost areas are significantly vulnerable to climate change. Thawing of permafrost decreases the stability of slopes and can affect infrastructure in mountain regions. The main factor affecting mountain permafrost is topography (Etzelmüller et al., 2009) and especially the topographic conditions influencing the incoming solar radiation. According to Gruber et al. (2009) there are two types of surface phenomena indicating the presence of permafrost in mountains - rock glaciers and other creep phenomena and hanging glaciers and ice faces. Damm et al. (2006) gives geomorphological indicators for mountain permafrost, among which are perennial snow patches. Perennial snow patches contribute to local permafrost occurrence and aggradation because they work as a shield with relatively high albedo, protecting the frozen underground from heat flux in summer. The existence of many perennial snow patches in an area in the mountains indicates a wider distribution of permafrost, especially in the shade of surrounding peaks (Haeberli, 1975; Rolshoven, 1982). Although there are high mountains reaching almost 3000 m in Bulgaria with suitable conditions for the presence of permafrost (Dobinski, 2005), there is low number of studies on this topic ~~(Onaca et al. (2020))~~(Onaca et al., 2020). No publications have been found to investigate the long-term state of the frozen subsurface in high mountains in Bulgaria.

With the development of modern technologies and in particular the equipment used in exploration geophysics, high-quality in-depth information can now be obtained. Geophysical techniques such as electrical resistivity tomography (ERT), and ground-penetrating radar (GPR) are widely used today for a multi-dimensional investigation of subsurface conditions in permafrost environments and corresponding landforms. Until the late 1980's, they were mostly applied in polar regions (see the review by

Scott et al. (1990)). The ERT technique is one of the basic methods for permafrost evidence and studies. Geophysical methods are applied also in glacial studies ~~and~~ with the GPR technique ~~is most important~~ used for the imaging of glacial subsurface conditions (Navarro et al., 2009) and internal glacial structure (Arcone, 1996).

The application of geophysical methods in mountain permafrost regions is related to changes of the physical properties of earth material mainly associated with the freezing of incorporated water. The degree of change in the physical properties depends on water content, pore size, pore water chemistry, ground temperature and pressure on the material (Hoekstra et al., 1973; King, 1984; King et al., 1988; Hoekstra et al., 1974; Scott et al., 1990). When applied on permafrost, most geophysical methods detect parameters correlated to ice content (Hauck et al., 2001) like high electrical resistivities ~~(ERT)~~(Yakupov, 1973).

Using geophysical methods, the structure, depth and extent of frozen areas beneath and near the snow field can be determined relatively quickly and easily, as well as the location of accompanying snow bodies and karst formations (Scott et al., 1990; Dimovski et al., 2015, Georgieva et al., 2019; Kisyov et al., 2018).

Ground-penetrating radar (GPR) is a high-resolution geophysical technique based on the propagation of electromagnetic ~~(EM)~~ waves. Dry snow and ice provide the optimal permittivity conditions of the radar signal from all possible geological environments for georadar pulses with a main frequency above $1\ MHz$. This is due to the extremely low degree of signal attenuation, which is a result of the low conductivity and the absence of any dielectric or magnetic relaxation processes above this frequency. The successful application of GPR in glaciology is related to the peculiar dielectric properties of frozen materials and to their large contrast with other geological materials (Evans, 1965; Fitzgerald et al., 1975). Employing high-frequency GPR antennas ($> 400\ MHz$) good results can be obtained in delineating the internal structure of perennial snow patches or permafrost zones (Annan et al., 1976; Berthling et al., 2000; Hinkel et al., 2001; Jørgensen et al., 2007; Gadek et al., 2008; Onaca et al., 2015). The advantages of GPR are that data acquisition and processing are relatively fast and the interpretation result can be focused on different depths and scales, with a variety of antenna configurations and frequencies (Pipan et al., 1999; 2000; van der Kruk et al., 2003; Jol, 2009; Zhao et al., 2015; 2016).

On the other hand, snow and ice are an ideal environment for exploration, as stratigraphically they are made up of horizons with good endurance and characteristic shapes. The ~~polar ice sheets may contain layers of basal sea ice several to hundreds of meters thick (?), while~~ glaciers from temperate continental belts may contain layers rich in dust, sand, or rock debris from a few millimeters to tens of meters (Arcone et al., 1995; Lawson et al., 1998). The perennial snow patches in high mountains are similar to mountain glaciers (as remnants of them) and also contain layers of rock material between thin layers of ice and firn (Kawashima et al., 1993).

Electrical resistivity method (ERT) ~~or 2D Electrotomography~~ is based on the changes in the electrical properties of rocks, both vertically and horizontally using different electrode circuits (Dimovski et al., 2007). Changes in electrical resistivity depend not only on changes in lithology but also in relation to the presence of water ~~in the cracks and pores of the rocks~~ (Dimovski et al., 2015;Hoekstra et al., 1973; Olhoeft,1978) in the cracks and pores of the rocks and its mineralization (Mares et al., 1984; Mares et al., 1984). The decrease in temperature leads to a decrease in electrolytic activity and hence a decrease in conductiv-

ity. This effect is significant below the freezing point. This is the reason why the ERT can successfully be applied for studying ~~glacial structures and frozen subsurface areas in mountain regions~~ permafrost areas (Kneisel et al., 2008).

A marked increase in resistivity at the freezing point was shown in several field studies (Supper et al., 2014; Hilbich et al.,
95   2009; Emmert et al., 2017; Hauck, 2013; Kneisel et al., 2007; Kneisel et al., 2008; Mauer et al., 2007; Ikeda, 2006; Hausmann et al., 2012; Onaca et al., 2015). In most permafrost materials, electrolytic conduction takes place, where the current is carried by ions in the pore fluids of the material. In poor conductors with few carriers, such as ice, a slight displacement of electrons with respect to their nuclei produces a dielectric polarization of the material, leading to displacement currents (Telford et al., 1990).

100   Even the GPR method gives a fairly accurate indication of ice thickness and ice internal structure and ERT is the main method used for permafrost investigations there are some limitations in using them in mountain regions and highly rugged terrain (Kneisel et al., 2008). A big limitation is the accessibility to the study site, the complicated logistics of bringing there the measuring equipment, and the safety during the work. Highly rugged terrain makes complicated GPR data processing (Annan, 1999) and needs complex mathematical corrections for relief and proper estimation of the velocity of pulse propagation.
105   The velocity is dependent on the dielectric properties of the media and particularly of the ice where it is a function of the temperature and water, ice, and air content. Mentioned inaccuracies can cause distortions in the spatial distribution of georadar data, registered boundaries, and, accordingly, the incorrect shape of the boundaries, the thickness of the individual layers and their actual depth. To minimize the inaccuracies the relief can be estimated using unmanned aerial vehicle (UAV) for example. The velocities can be estimated using reference values from boreholes or by producing a velocity model based
110   on the radargrams. ERT is limited in applying in sites covered with coarse gravel or when a thick ice layer is present (Kneisel et al., 2008). In the first case, the consequence is a bad contact between electrodes and the rocks while in the second case the very high electrical resistivity of ice can hinder the measurements. Distortions in estimating subsurface structure can be met in highly rugged terrain due to inaccurate estimations of the surface and measurement geometry. Interpretation of ERT and GPR data can also be ambiguous and consequently is advisable to use more geophysical methods on one site (Kneisel et al.
115   , 2008; Hauck et al., 2001).

In 2018, 2019, and 2020 geophysical measurements including GPR, 2D ERT, very short meteorological record and surface capture with a UAV were conducted by the ~~team in two places in Pirin Mountain -~~ authors and a team of students in Golyam Kazan cirque ~~and Banski Suhodol valley~~, Pirin Mountain. The aim was to investigate the thickness, internal structure of ~~perennial snow patches and~~ the Snezhnika microglacier, and the subsurface structure near ~~them. Geophysical measurements in~~
120   ~~Golyam Kazan cirque were made in three consecutive years and results are presented in thispaper.~~ it (within the glacial bed). Even though this glaciarret is monitored since 1994 (Gruenewald et al., 2008) the information on the ice thickness is very poor and one point of our work was to solve this. Knowing the thickness of the microglacier at many points is needed to estimate the ice mass. Further measurements of its size and thickness will allow being monitored the mass balance of Snezhnika and then determine the relationship between the change in meteorological parameters (or climate if the monitoring is made long enough)
125   and the change in ice mass. The second point was to investigate where the meltwater from Snezhnika disappears beneath the microglaciers' bed. The results from our study are presented in this paper.

2 Methods

Geophysical measurements near Snezhnika microglacier include ground penetrating radar (GPR) and 2D Electro Resistivity Tomography (ERT). GPR profiles are crossing the microglacier, while ERT profiles lie between the ice body and the front moraine. Digital elevations model (DEM) with resolution 7.63 cm/pix was also constructed using drone photogrammetry.

2.1 Study site description

Pirin Mountain is a crystalline horst which is part of Rila-Rhodope massif located in southwestern Bulgaria. The studied site is situated in the northern part of the mountainNorthern Pirin, around the highest peak Vihren (2914 m). The This part of Pirin mountain consists mainly of marble that makes up the steep ridges and lends the relief its characteristic appearance (Boyadjiev, 1959). It has been subject to cryogenesis and karstification since the glaciers retreat (Gachev, 2017b; Gachev et al., 2019).

Snezhnika microglacier (Gruenewald et al., 2008)is situated in the Golyam Kazan cirque, in Pirin Mountain, noted as the southernmost perennial snow patch microglacier in Europe (Grunewald et al., 2010; Gachev2017a), 2017a), is situated in the Golyam Kazan cirque. The location of Snezhnika is determined by the morphological features of the Golyam Kazan cirque, formed between the eastern slope of Vihren Peak (2914 m) and the southern slope of Kutelo Peak (2908 m) (Fig. 1), at around 2400 m asl. It is open to the east, with dimensions of 1200 by 1250 m and an surface of about $1.2\ km^2$. The western and southern parts of the cirque are outlined by the steeper slope of Vihren Peak and Dzhamdzhiev ridge. The morphology of this slope, and in particular the morphology of the Vihren wall, at the base of which the snow patch glaciarret is located, favors the accumulation of snow masses through avalanches and shading. The Vihren wall rises west of the snow patch microglacier and 420 m above its surface. The wall has mainly eastern exposure and partly northern exposure with slopes from 55 to 65° (almost half of its area). The largest slopes, reaching in places from 85 to 90°, are characteristic of the lower part of the wall. They The steep slopes were formed during the final phase of the last (Wurm) glaciation (Popov, 1962, 1964).

Vegetation in Golyam Kazan cirque is with low coverage and belongs to the alpine and subalpine zone. Vegetation is presented mainly in central part of the cirque and is almost absent in the area of the microglacier. There are no surface water, lakes or rivers, in the cirque. Pirin Mountain is on cross-roads of Mediterranean and Continental climate. Snow cover in the mountains of South-West Bulgaria is present for 180-200 days yearly. The mean maximal thickness of snow is about 180 cm and the absolute maximal thickness measured until 2005 is about 350 cm (Brown et al., 2007).

The size of Snezhnika microglacier varies from year to year as it is visible on can be observed in Fig. ?? 2 but no trend can be determined (Gachev, 2016). Therefore, it cannot be said whether its size decreases or increases starting from the first measurements in 1994 (Gachev, 2016). During the period in which the presented study was conducted (2018-2020) the size of Snezhnika decreased. This made it possible to make ERT profiles on in the same place in over the microglacier's bed where the GPR profiles were made in the previous year.
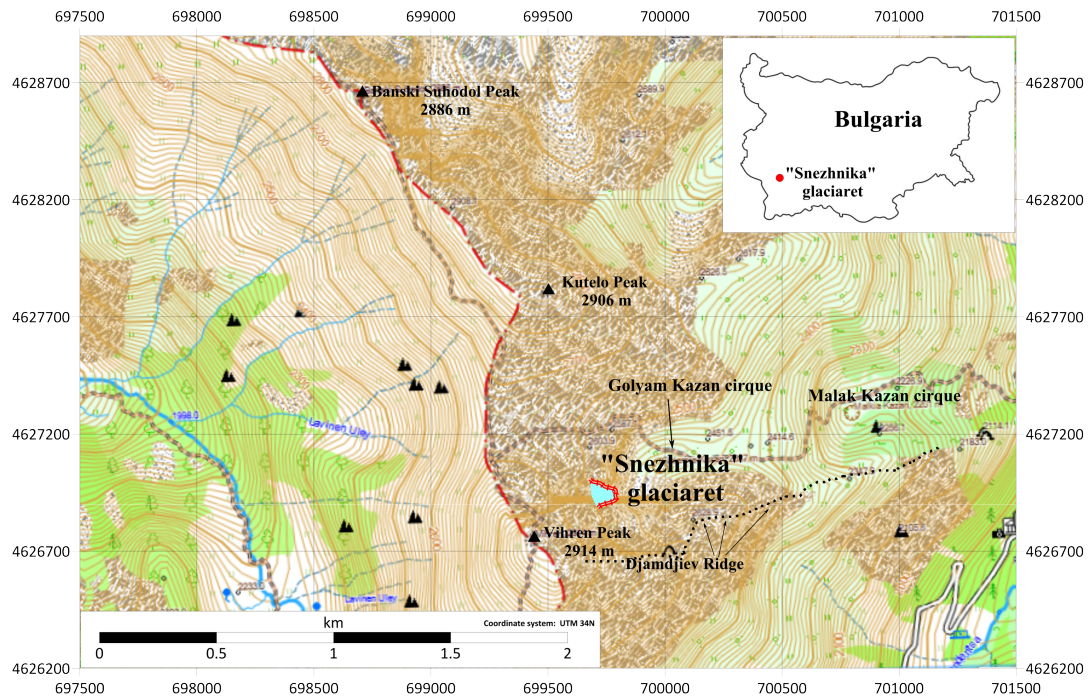
Figure 1. Snezhnika microglacier in Golyam Kazan cirque, surrounded by the highest peaks in Pirin Mountain - Vihren and Kutelo. ~~Picture On the northern side of the cirque~~ is ~~taken from~~ Dzhamdzhiev ridge, which starts from the Vihren peak and ends in the valley near the Banderitsa hut. Map base layer is provided by karta.bg.

2.2 Ground-penetrating radar

Measurements in Pirin Mountain were carried out using a GPR system, including a SIR-3000 control unit and $270\ MHz$ antenna model 5104A by GSSI, Inc. USA. The settings used are listed in Table 1. By default, all radargrams are processed with the following processing levels:

- Pre-processing and geometrization of the radargrams (profiles lengths adjustments; orientation flip; declipping of extreme values and multiplying by scaling factor 1.44; dewow by subtracting mean value at 4 ns time window; resampling the data in x-direction by 2.5 cm trace increment; fixing the zero level by cutting the time section where waves pass through the air before the ground surface)

- Standard filtration and smoothing (cosine-tapered bandpass filter with low cut frequency 50 MHz, lower plateau 75 MHz, upper plateau 550 Mhz and high cut frequency 750 MHz; 2d median xy-filter on a 5 traces by 5 samples window)

- Signal amplification (profiles normalizing by energy equalization of the parallel profiles; profile trace normalize in order to produce mean amplitude equality distribution for all traces)

- Eliminate horizontal reverberations (applying a background removal filter)
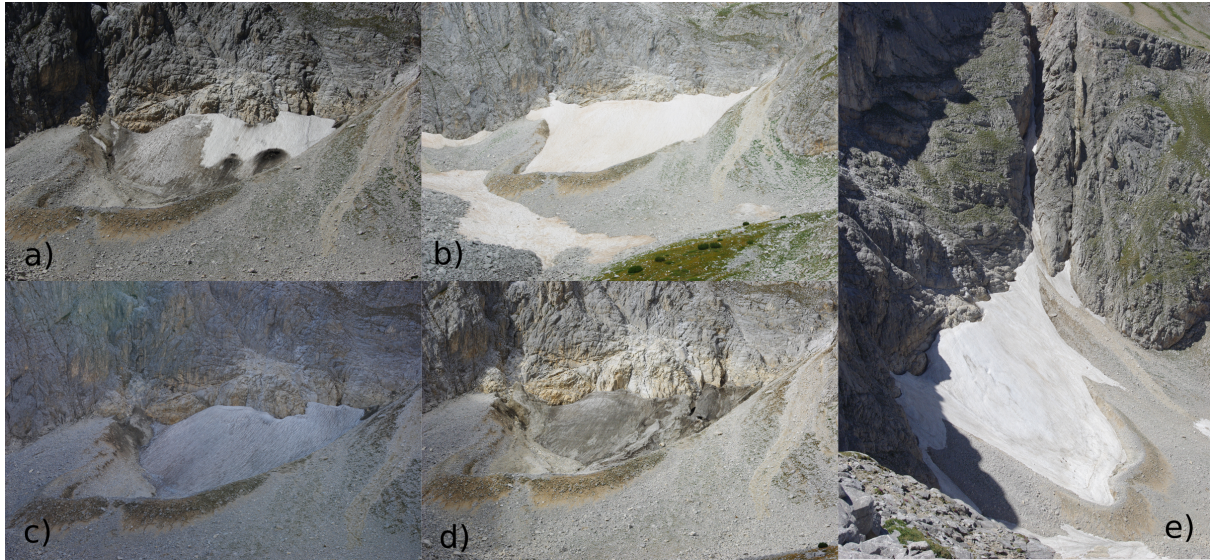
Figure 2. Snezhnika microglacier in Golyam Kazan ~~in~~ over the years (a) 2017, August 25; (b) 2018, August 25; (c) 2019, October 5 and (d) 2020, October 9. ~~Well visible is decrease of its size between 2018 and 2020 when geophysical measurements were made.~~ Picture e) is taken from the Dzhamdzhiev ridge (near Vihren peak) on 01 July 2017. The shading of the ridge is already visible.

Table 1. GPR Settings of the measurements.

SURVEYPARAMETERS	2018	2020
Scans per meter	40	20
Samples per scan	1024	512
Time window	210 ns	300 ns
Automatic gain	4 pts	4 pts

IIR Filters Vertical: LP = 700 MHz HP = 75 MHz

For inverting and interpreting of GPR data the following generalized lithological media with their estimated mean velocities taken from standard properties tables were used in the radargram models: ice 0.15 m/ns, gravel with ice 0.13 m/ns, limestone 0.12 m/ns (Baker et al., 2007).

GPR profiles within this study were made in 2018 and 2020. Locations are presented ~~on~~ in Fig. ~~4. Coordinates of profiles~~ 3. Profile coordinates were recorded with Garmin GPSMAP 64st and Garmin GPSMAP 66s with error in horizontal coordinates $1-2\ m$. The exact positions of the profiles were then evaluated from UAV images and the accuracy was improved. All profiles from 2018 are perpendicular to the slope and follow the ~~relef~~relief's horizontals. The first one - GPR(2018)-01, is located in the lowest and comparatively flattened section of the microglacier, and the last, GPR(2018)-05, was in the highest elevation area accessible without additional security. Two profiles from 2020 were situated along the slope and two were in the lower

part of the microglacier's bed between head moraine and ice. ~~In 2018 this area was covered by snow (Fig. ??). In order to~~ ~~simplify the processing and the interpretation, all radargrams, except~~ The two profiles along the slope (GPR(2020)~~3~~ 1 and GPR(2020)~~-3, have no topography and are with zero reference level in the elevation axis. The location of the profiles parallel to the slope~~ 2) allowed determining the depth of the ice in the upper parts of the ~~snowfield. Due to the steep slope, laying~~ ~~profiles perpendicular to the slope in this part is extremely difficult.~~ glaciarret. There is no repetition of the GPR profile within the two years. Efforts were made to cover more microglacial area with GPR data and to estimate its thickness in more places. The second reason is that most of the GPR profiles from 2018 were not part of the microglacier in 2020.

2.3 Electrical resistivity method

Based on ~~the measurements~~ other surveys conducted in different areas of Europe (Supper et al., 2014; Hauck et al., 2001; Mauer et al., 2007; Ingeman-Nielsen, 2005), we determined the most suitable parameters of the measuring scheme for optimal results ~~with~~ when observing permafrost. Measurements in Pirin mountain were carried out using 24 electrodes connected to a resistivity meter (ABEM SAS 1000). The ~~measurements were obtained by combinations of systematic changes in the~~ ~~location of the four active electrodes~~ field measurements were performed utilizing a four-electrode Schlumberger array. The multi-electrode resistivity technique consists in using a multi-core cable with 24 conductors, as electrodes plugged into the ground at a fixed spacing. In the resistivity meter itself are located the relays which ensure the switching of those electrodes according to a sequence of readings predefined and stored in the internal memory of the equipment. The various combinations of transmitting (A, B) and receiving (M, N) pairs of electrodes construct the mixed sounding/profiling section, with a maximum investigation depth which mainly depends on the total length of the cable. The lengths of the profiles were chosen to have the maximum length and depth of study, while not having to cross over the moraine ridge of the microglacier (which was unstable and dangerous for climbing). Profiles are around $30-40\,m$ long with north-south direction and electrode spacing of $1.5\,m$. The depth of the study depends on the distance between the electrodes and the geometry of the circuit, the gradual increase of distance makes it possible to increase the depth of the subsurface study. In our study, a maximum depth of $9-10\,m$ is reached, and for most of the profiles the expected depth at this length of the measuring line with ~~a~~ the multi-electrode system ~~with 24~~ ~~electrodes using the fore-electrode symmetric Schlumberger array,~~ was $6-7\,m$. The selected length of the profiles and the type of measuring scheme were in accordance with the conditions ~~on the field~~ in the field (namely the width of the glacier bed and the save access to the first and last electrodes), and the impossibility of applying a three-electrode (pole-dipole array) or dipole-dipole array measuring scheme. ~~The lengths of the profiles were chosen to have the maximum length (through the~~ ~~whole microglacier bed) and depth of study, while not having to cross over moraine ridge of the glacier (which was unstable~~ ~~and dangerous for climbing). Profiles are around $30-40\,m$ long with north-south direction and electrode spacing of $1.5\,m$.~~

ERT measurements near Snezhnika were conducted in 2018, 2019 and in 2020 along one, two and three profiles respectively. They were situated in the lower part of the microglacier~~bed on the free from~~'s bed on an area without any ice and snow ~~area~~ cover (depending on the size of microglacier in the respective year Fig. ~~??~~2). Thus the first profile was measured all three years, the second twice and the third only in ~~2020 (Fig. 4).~~ 2020. The last profile crosses small part of the microglacier (Fig. 3). A pseudo-section of the apparent resistivity for each profile was ~~obtained, consisting~~ then obtained. It consists of the
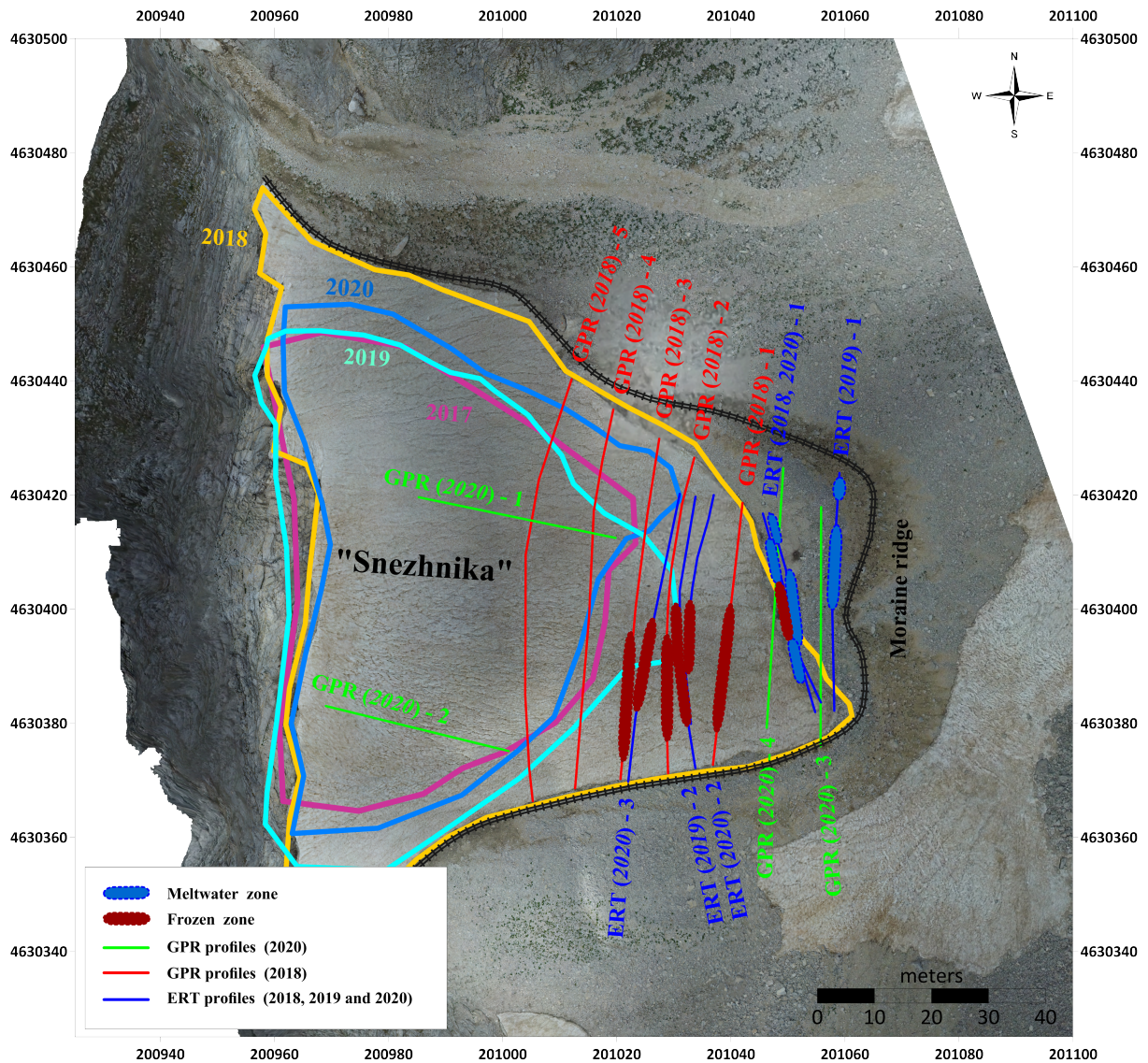
Figure 3. Location ~~and direction (labels are on the starting point)~~ of the all GPR (red for 2018 and green for 2020) and ERT (blue) profiles in ~~Golyam Kazan~~ Snezhnika area. ~~Error in horizontal coordinates~~ The size of the ~~profiles~~ glaciarret between 2017 and 2020 is ~~1 — 2 m~~ given with lines in different colors. Bold red lines show the position of ~~frozen subsurface areas~~ permafrost area, and bold blue lines show place of melt water (subsurface drainage system). The background picture is made with the UAV in 2018 in the same day of measurements.

measured values at certain points along horizontal lines at a certain depth. ~~To transform it into a real geoelectrical section, we used the algorithm for two-dimensional~~ In order to obtain a model of electrical resistivity a least squares inversion by the method of ~~least squares~~ quasi-Newtonian optimization, proposed by ~~Loke et al. (1996), implemented by quasi-Newtonian optimization~~ (Loke et al., 1996), was implemented and the pseudo-section was transformed into a real geoelectrical section.

In addition to the both main geophysical methods a digital terrain model (DTM) of Snezhnika with resolution 7.63 cm/pix was produced using UAV photogrammetry. The elevations in the study are taken from topographical maps in scale 1:5000, from produced DTM and the GPS data.

220   Measurements were made on 25 August 2018, 4-5 October 2019, and 8-9 October 2020. It was not possible to work on the same date every year for many reasons, the most important of which is the weather in the mountain. The time of measurements was chosen to be at the end of the summer and before the first snow in the mountain when the size of perennial snow patches is expected to be the smallest. This is a relative time because in one year the first snow falls in September (like it was in 2017 and 2018) and in the other, the weather in October is still warm (October 2020).

3   Results and discussion

3.1   ~~Geophysical investigations of Snezhnika microglacier~~

The thickness and internal structure of the Snezhnika microglacier were investigated using GPR. ~~The obtained GPR data were used to acquire nine radargrams~~ We acquired nine radargram, which were analyzed and interpreted and are presented ~~on~~ in Fig. ~~6~~4, Fig. ~~7~~5, Fig. ~~5~~6. Across seven ~~radagrams~~ radargrams the discontinuity between the microglacier's ice and bed is well

230   visible. ~~The~~ On the other two profiles ~~were made in the lowest part of microglacier's bed~~, situated in a free from ice area ~~and respectively the~~, this discontinuity is not presented respectively.

   ~~On~~ In the Fig. ~~6~~4 are presented radargrams from 2018, which are horizontal relative to the slope. The ~~snowfield is situated in a very steep area and this made measurements in its upper part very difficult. The~~ uppermost layer represents the microglacier. Its depth varies between $1-2\,m$ in the lowest part (Fig. ~~6~~4a) and $5-6\,m$ on the last profile (Fig. ~~6~~4e). ~~Within the ice, there are~~

235   ~~some less differentiated discontinuities, probably related to the structural features of the ice body. For this layer an average ice velocity of $V_{ice} = 0.15\,m/ns$ was used (Baker et al., 2007). The place of~~ In 2018 the size of microglacier was bigger than in 2017 (Fig. 2a and Fig. 3) and accordingly its lowest part consists of the "new" snow left from the last winter. This are profiles GPR(2018)-1, GPR(2018)-2 and partially GPR(2018)-3 (Fig. ~~6~~4a,b and c) ~~was not covered by snow in previous year (Fig. ??a) so~~. Within the first layer ~~of these three profiles, respectively, is actually the "new" snow left over from the last winter~~, there

240   are some less differentiated discontinuities. Probably they are related to the periods of accumulation of the snow in winter, avalanches and periods of warm and cold weather during the winter of 2017/2018 when the melting and freezing occurred forming thin ice crusts.

   The second layer lies under the snow and the ice, representing the glacial bed ~~of rock blocks of different sizes, the voids between which~~ which consists of cobbles and pebbles. The voids between them are filled with ~~ice and water~~ water and this

245   area has low resistivity values on ERT profiles. We presume that this layer is draining the melted glacial water. The thickness of this layer varies from 1 to $4\,m$ along the particular lines and its depth is between $3.5-6\,m$ on the first profile (Fig. ~~6~~4a) and $5-8\,m$ on the last one (Fig. ~~6~~4e). ~~An average layer velocity of $V_{gravel} = 0.13\,m/ns$ is used.~~

   The third layer has a complex topography in the lower elevation survey lines, while in the higher elevation lines (GPR(2018)-03, GPR(2018)-04 and GPR(2018)-05, Fig. ~~6~~4 c,d and e) it becomes almost parallel to the one above with a thickness of
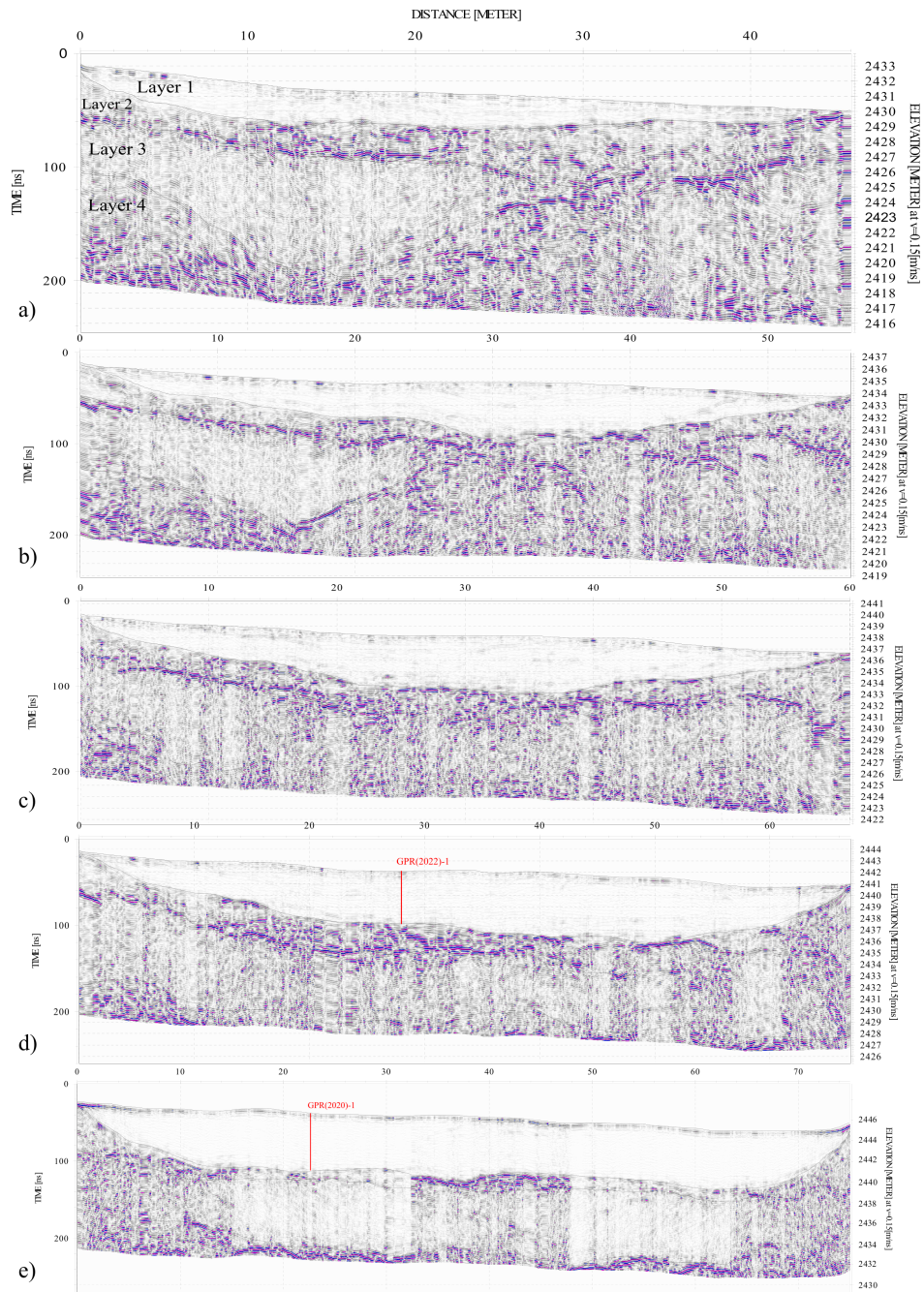
Figure 4. GPR profiles from 2018: a) GPR(2018)-1 situated at lowest altitude; b) GPR(2018)-2; c) GPR(2018)-3; d) GPR(2018)-4; e) GPR(2018)-5 situated at highest altitude. All profiles are with horizontal elevation. Red lines indicate the ~~coss~~ cross point with GPR(2020)-1.

Figure 5. GPR profiles from 2020 along the slope of Snezhnika: a) GPR(2020)-1 north; b) GPR(2020)-2 south. Red lines indicate the cross point of GPR(2020)-1 with GPR(2018)-4 and GPR(2018)-5.

250   $4 - 6$ m. In the first and second ~~survey line~~ profiles (GPR(2018)-01 and GPR(2018)-02), the layer is relatively thin in its central part (about 1 m), while two pocket-like recesses with thickness of up to about $6 - 7$ m (and depth $10 - 12$ m from the ground level) are formed along the left ~~and the right~~ part. The presence of ice causes ~~some distortion of the signal due to large differences in the velocity~~ a decrease of reflections of electromagnetic waves ~~in dry and icy areas. Based~~ and based on this we assume that the pocket-like structures are ice lenses ~~. The intermediate layer velocity used in the interpretation is~~
255   ~~$V_{limestone} = 0.12$ m/ns~~or ice-rich area.

Pale rectangular areas are visible on the radargrams. Most visible they are on the higher elevation profile (GPR(2018)-05, Fig. ~~6~~5e). They have no scientific meaning and ~~exist due to technical reasons. Due~~ are the result of technical difficulties due to the steep slope in the upper part of the microglacier~~the~~. The measurements were stopped and started several times and this caused gain level changes in some places.

260   ~~On Fig. 7 profiles GPR(2020)-1 and GPR (2020)-2 along the slope of Snezhnika are presented (Fig. 4). Both profiles are plotted horizontally in order to present better the discontinuities, although there is a change in elevation of 24 m between start and end point of each profile. In the both radargrams only the icelayer can be seen.~~

In 2020 two more GPR profiles were made on Snezhnika in order to add more information about the thickness of the ice. The first profile (GPR(2020)-1, Fig. ~~7~~5a) clearly outlines the lower surface of the ~~snowfield~~ glaciarret with a depth of between 4 and
265   7 m. At the beginning of the profile (left part of radargram), fading of the phases is observed at a greater depth (> 7 m), which may be due to a frozen zone beneath the upper part of the microglacier. In the first half of the radargram a hill-like structure

is visible, which ~~can be~~ is interpreted as plucking zone of the microglacier. On the right part of the profile the discontinuity between the microglacier's ice and the bed has the greatest depth of $7\ m$, which becomes shallower at the end of the profile, in the last $4-5\ m$ of it. Beneath lowest part of the microglacier another hill-like structure is visible. It can be interpreted as the new head moraine.

In the second profile (GPR(2020)-2, Fig. ~~7~~5b), the relief of the lower surface is clearly traced at a depth of about $8\ m$. Here a layer with a depth of 4 to $8\ m$ is distinguished, which is composed of either frozen and well-joined rock blocks or older ice. At the lower end of the profile (right part of the radargram), single reflections can be ~~seen~~ observed in this layer, ~~which are probably due to larger pieces of rock~~ caused by boulders covered by ice.

The obtained depths of the Snezhnika in 2020 correlate very well with the results obtained in 2018. At that time, the depth in the uppermost profile is about $6-7\ m$ (Fig. ~~6~~4e). Profile GPR(2020)-1 intersects profiles GPR(2018)-4 and GPR(2018)-5 and as can be seen from Fig. ~~4~~3 and Fig. ~~7~~5a the place of intersection is also the place of the greatest thickness, with a depth of $7\ m$. The deepest part of microglacier is detected on GPR(2020)-2, where the thickness of the ice is $8\ m$. This profile is located in the southern part of microglacier, which is most shaded by Vihren wall and Dzhamdzhiev ridge (Fig. ~~??~~2e). The effect of shading is also well visible on Fig. 4a where the snow layer is thicker in the southern part of the profile. The obtained maximal thickness of microglacier shows agreement with results from early borehole measurements conducted by Popov (1962). The depth of 11 m (Gruenewald et al., 2008) is not detected even with wider aerial information obtained from geophysical measurements. We have to notice that borehole measurements of depth give only point information, compared to the profile measurements, and not the whole area of microglacier was covered by GPR profiles in years 2018 and 2020. Onaca et al. 2022 measured a depth of the border between ice and gravel of 12 m in a small area in the upper part of the microglacier, which is probably the maximal estimated thickness of Snezhnika. GPR profiles made within the presented study don't cross this area. This indicates a necessity of using a thicker net of GPR profiles in the future to map better the lower border of the microglacier.

The main layers outlined in the study area are also presented in Table 2.

3.1 ~~Subsurface structure of microglacier bed~~

Subsurface structure of microglacier bed was investigated using ERT and GPR measurements. On Fig. ~~5~~6 are presented two GPR profiles from 2020, located in the ~~lowest~~ lower in elevation part of the investigated area (Fig. ~~4). A change in elevation between these horizontal relative to the slope profiles can be observed, which is due to the topographic correction during the GPR data processing. The elevations are taken mainly from topographical maps in scale 1:5000, from DEM based on aerial photography and GPS data. In the presence of relatively uniform inclination of the profile line relief is introduced as a linear function of the start and end points of the profiles.~~ 3).

The two GPR profiles situated in the glacial bed were also covered by ERT measurements. Fig. ~~??~~7 shows pseudo-section of the ~~apparent resistivity for profile ERT-PR1~~resistivity values for profile ERT(2018,2019,2020)-1, measured in 2018, 2019 and 2020. On the resulting plot, three zones can clearly be distinguished. Zone-1 is situated near the surface and represents ~~gravel with different size of rocks (between 1 mm and $15-20\ cm$) It~~ a mix mainly of pebbles and cobbles. It is characterized by a relatively high electrical resistivity of 8000 to $40000\ \Omega m$ which ~~is typical~~ are typical values for broken marble rocks (Dortman,

Table 2. Description of the stratigraphy of the study area.

Layer	Depth	Thickness	Description	GPR velocity
1. Microglacier	From $1-2\ m$ in the lowest part and up to $7-8\ m$ in the higher part	2 to 8 m	The top layer combines the inner sublayers and discontinuities of the microglacier	$0.15 m/ns$
2. Glacial bed	Between $3.5-6\ m$ in the lowest part and $5-8\ m$ in the upper parts of the slope	1 to 4 m	Rock blocks of different size with voids and channels between them filled with ice and water	$0.13 m/ns$
3. Permafrost	7 to 9 m in the lower parts of the relief with two pocket-like recesses up to $7-9\ m$ and between $11-13\ m$ in the higher parts	1 to 8 m	Permafrost zone with two ice lenses along the left and the right side under the glacial bed of the microglacier	$0.15 m/ns$
4. Bedrock	$>14\ m$	$>10\ m$	Fractured marble rocks massif	$0.12 m/ns$

1984). In 2018 (Fig. ??7c) the thickness of this zone is $1.5-2\ m$, and in the next two years it reaches up to 4 m (Fig. ??7a and b). Below the first zone, at a depth of 1 to 5 m, the second zone is located (Zone-2). It is characterized by relatively low values of the specific electrical resistivity within the range of 1000 to 8000 Ωm. This zone represents a highly watered zone, draining the melting microglacier water. Its size is smaller in 2018 and is located mainly in the edges of glacial bed on a depth of 3 m.

305 In the next two years its size increases and its thickness decreases to 2 m. The deepest zone (Zone-3) is of the greatest interest and is characterized by resistivity over 60000 Ωm. High resistivities (Kneisel et al., 2008; Hauck et al., 2001) are typical for ice and frozen subsurface. Based on this we assume that the zone represents a frozen area . permafrost and respectively the Zone-3 represents an ice-rich permafrost area.

In 2018 the melt water was drained around the frozen subsurface areas in the lower part of Snezhnika in Zone-2. In 2019
310 and 2020 the size of the glaciarret was smaller and this obstacle no longer existed or was deeper than it was reached from ERT method. Then the main flow of meltwater was directed below the central part of the microglacier's bed. Profile ERT(2019)-1 is situated 5-6 m lower at elevation from profiles ERT(2018)-1 and ERT(2020)-1 (Fig. 3). On this profile, the lowest resistivities in Zone-2 are observed. Probably the melt water is collected in this area in the lowest part of the microglacier's bed and then it flows deeper through a karst structure. We can assume this because the area is very close to the head moraine, but no surface
315 water is observed on the opposite side of the moraine or down along the slope.

In the second electrical profile (ERT-PR2ERT(2019,2020)-2), presented on Fig. ??8, we distinguish two zones. Zone-2 is located in nearsurface area of the profile, with a thickness up to 2 m. This area represents the accommodating medium composed of crushed marble pieces of different sizes(as the marble is the main rock type in the area), having a resistivity between 10000 and 40000 Ωm. The zone is highly watered and is a result from melting of the microglacier. In the southern part of the
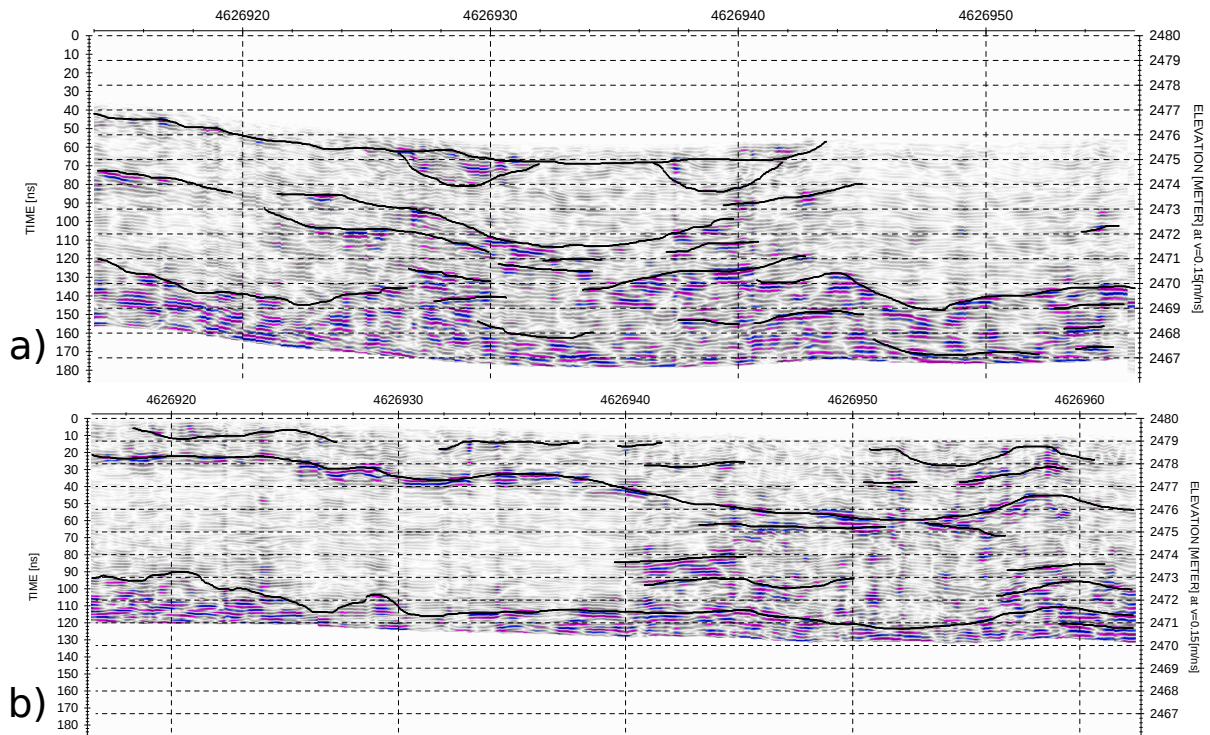
Figure 6. GPR profiles from 2020 situated in glacial bed near the head moraine: a) GPR(2020)-3; b) GPR(2020)-4.

320   profile at a depth beyond the third meter in the section Zone-3 is located. This zone appears with values of electrical resistivity over $60000\ \Omega m$ and represents ~~a frozen~~ an ice-rich permafrost area in the base of microglacier. In 2020 (Fig. ~~??~~8 down) the frozen area is located about $1\ m$ deeper than in 2019 (Fig. ~~??~~8 up). In October 2019, there was much less precipitation in the area (below average) and slightly lower air temperatures than in October 2020, when air temperatures were higher and the precipitation was above average (based on Copernicus Climate Change Service reports). This may have led to an increase in

325   the active layer thickness in 2020. Another reason for this change is that the two profiles do not exactly match in location. Although they are quite close to each other, the small displacement may be the reason for the greater change in depth. Probably the sinking of the permafrost area in 2020 compared to 2019 is a result of two factors - interannual change of the meteorological parameters and the shift of the location of the profile.

    Fig. ~~??~~ 9 shows the third ERT profile (~~ERT-PR3~~ERT(2020)-3), located just below the ~~glacier~~glaciarret). This profile was

330   measured only in 2020 when the size of Snezhnika was the smallest. The measuring line passed through a small piece of the ~~snowfield~~microglacier, which is well seen on the Figure. Only one electrode was in the ice, which was covered by a thin debris layer, and this probably made the measurement possible. Zone-3, representing again the ~~ice~~ice-rich area in the base of the microglacier, occupies a large part of the section. It is located at a depth of $4\ m$ in the southern part of the profile and in the
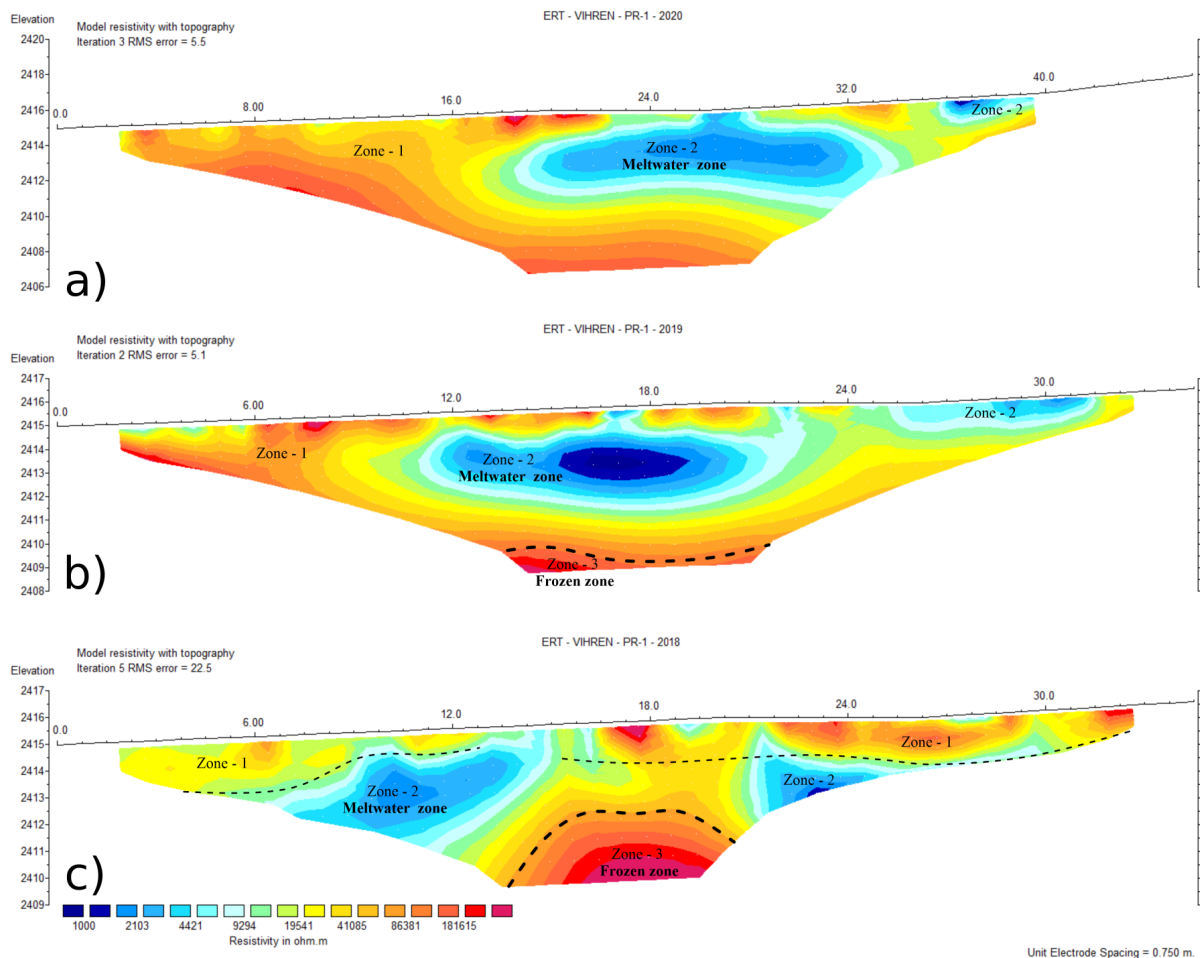
Figure 7. Electrical resistivity sections along ~~ERT-PR1~~ ERT-1 obtained near Snezhnika microglacier in 2020 (a), 2019 (b) and 2018 (c). Blue color represents low resistivities and red color indicates areas with very high resistivities.

northern it reaches the surface. Namely the northern part of the profile crosses part of the ~~glacier~~ glaciarret (Fig. ~~4~~3). Zone-2 on ERT-PR3 is distinguished only in the very shallow parts of the profile.

~~The frozen subsurface area and zone of draining water are better seen when we compare radargrams and ERT plots. Comparison is presented on Fig. 8 and Fig. 10.~~

~~ERT-PR1 and GPR(2020)-3 profiles. Black arrows show water channel. Dashed arrow shows frozen area.~~

~~ERT-PR2 and ERT-PR2 profiles and GPR(2018)-1 and GPR(2018)-2 profiles from 2018. Black arrows show the frozen zone.~~

On the ~~resulting plot for ERT-PR1 and GPR~~ aligned GPR and ERT profiles shown in Figure 10 the permafrost area and drainage layer of melt water are better visible. The Figure presents the alignment of profiles ERT(2020)~~-3, frozen and watered zones can clearly be distinguished (Fig. 10). Position of these zone on radargram is shown by arrows. The watered zones have~~
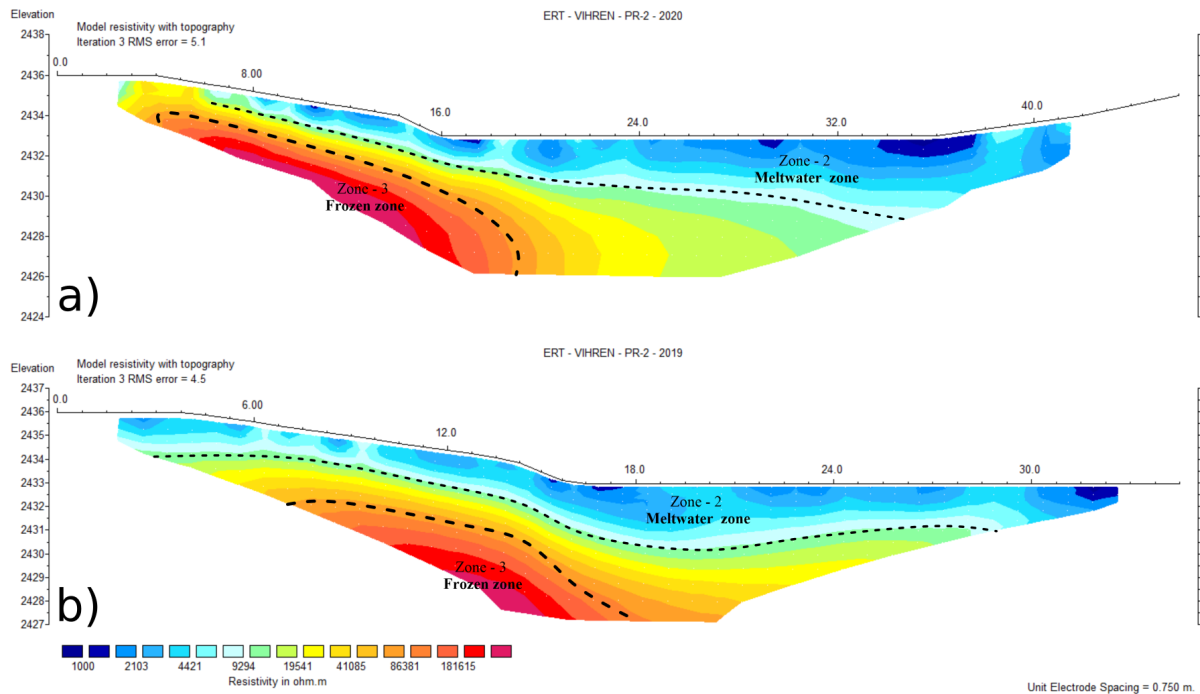
Figure 8. Electrical resistivity sections along ~~ERT-PR2~~ ERT-2 obtained in Golyam Kazan area in 2020 (a) and 2019 (b).
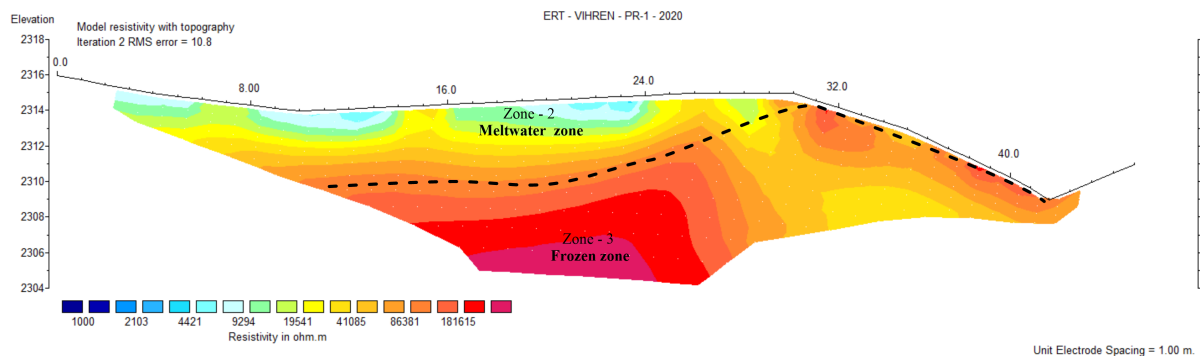
Figure 9. Electrical resistivity sections along ~~ERT-PR3~~ ERT-3 obtained in Golyam Kazan area in 2020.

~~low values of resistivities and more reflections on GPR profile. They represents areas formed by the melting of the glacier,~~
345 ~~mixed with crushed rock material. Between them is situated a zone characterized by high resistivities of more than 60000 Ω*m*~~
~~on ERTplot and a phase fading on GPR plot, representing the frozen area at the base of the microglacier.~~

~~Figure 8 shows ERT-PR2 profile measured in 2019 (up, left) and in 2020 (down, left)~~-2 and GPR(2018)-1 and ~~GPR(2018~~profiles
ERT(2019)-2 ~~profiles. Snow layer from 2018 is well visible on the radargrams (right on the figure)and~~ and GPR(2018)-2. The
two ERT profiles are located between GPR profiles and are shifted by several meters. Although the surface beneath the snow
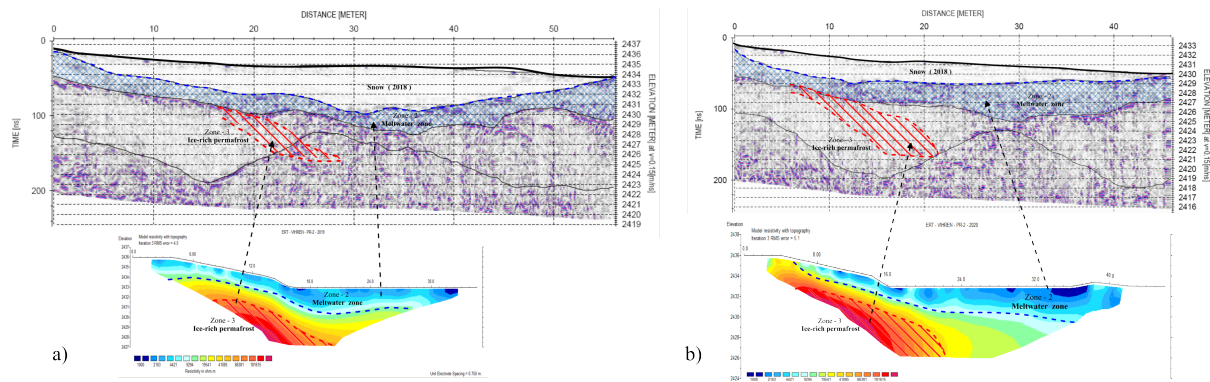
Figure 10. Aligned profiles ERT(2019)-2, ERT(2020)-2, GPR(2018)-1 and GPR(2018)-2. The red-shaded zones have the same size on ERT and GPR profiles to show areas of overlapping for permafrost zone. Blue-shaded areas present the layer draining the meltwater.

350 ~~has the same shape~~ on GPR profiles has the similar shape as the surface on the ERT profiles without snow. ~~ERT data cover smaller area in depth than GPR although~~ On the aligned plot the high resistivity zone fits well with the area ~~of frozen zone interpreted on GPR profiles~~ identified as ice rich permafrost on the GPR profiles. This zone is observed on both GPR(2018)-1 and GPR(2018)-2. Over the next two years, ERT(2019)-2 and ERT(2020)-2 profiles show very high resistivities at the site where the permafrost zone was observed. In the figure, these zones of overlap are shown with a red-shaded area on radargrams.

355 ERT profiles have shorter lengths and smaller depths and allow us to explore only part of the permafrost area. Some changes in the depth and expansion of the zone during the period (2018-2020) can also be observed. But until the profiles don't overlap exactly, it is difficult to analyze the reasons for these changes and we can only suggest this finding be investigated more during future measurements in the area.

~~The~~

360 The study presented includes measurements made over three consecutive years and a frozen zone is observed every year. As permafrost is defined as subsurface area the temperature of which remains below 0° for at least two consecutive years (Harris et al., 1988) or in our case the presence of ice this can be treated as evidence of permafrost existence in high mountains (particularly Pirin Mountain) of Bulgaria.

Permafrost is presented by a zone with a lack of reflections on GPR, which allows us to assume that this is ice-rich
365 permafrost. It might be a remnant from Snezhnika when it has a bigger size for several consecutive years, followed by a long warm period of debris accumulation over the ice.

Our results show that the permafrost zone is situated mainly in the southern part of the microglacier's bed (Fig. ~~4~~3). Also, the southern part of the microglacier is at least 1 m thicker than the northern one (Fig. ~~7~~5). The snow layer in 2018 is also thicker in the southern part (Fig. 4a). The reason is that this part is closer to Dzhamdzhiev ridge and the wall of the Vihren
370 peak - both with very steep slopes and rising 300 - 400 m above the surface. They shade the Snezhnika for most of the day~~even in the sunniest days of summer, as seen from Fig ??~~, as it is visible in Fig 2e. The picture is taken namely from ~~Dhamdzhiev~~

Dzhamdzhiev ridge on 1. July in the middle of the day and the shadow over the southern part of the microglacier can already be observed. The shading effect causes the northern part of the area to be exposed to the sun longer than the southern part. During the summer this protects the microglacier and the ~~frozen area from high temperatures~~permafrost area decreasing solar
375 radiation. Proof of this assumption is the presence of snow patches, located at the bottom of the Dzhamdzhiev ridge, close to the Snezhnika. Snow patches ~~were no~~ are not observed in the northern part of the cirque. ~~From the other side, no frozen zone was obtained near the perennial snow patch located in the middle of the Banski Suhodol valley, Pirin Mountain (unpublished research of the authors). The valley is situated northern from Golyam Kazan cirque and is more wider than it, thus the shading from the surrounding mountain ridges is less.~~

380 The ~~frozen zone in Golyamm~~ permafrost zone in Golyam Kazan cirque was obtained in 2018 on the ERT profile and in GPR profiles PR(2018)-1 and GPR(2018)-2. The ~~results from~~ 2020 ~~are showing again~~ results again show indications of a frozen area below the surface, although its ~~lower part is not discovered~~ upper part was not found at the same depth as in 2018. ~~The One~~ reason for this ~~is~~ may be the smaller size of Snezhnika in 2020 compared to 2018. The ~~perennial snow patch~~ glaciarret preserves the frozen subsurface area in summer. Even when the size of the microglacier is smaller, a ~~frozen~~ permafrost zone
385 exists but is observed more deeply. ~~The shading of surrounding mountain ridges~~ This change in depth is probably due to several factors such as the lack of shading from glaciarret, the interannual changes in meteorological parameters between 2018 and 2020, and the shift of the GPR and ERT profiles between the campaigns. The role of the shading of the surrounding mountain is also important but probably is less effective than ~~protection of snowpatch, but it is very important.~~

~~The study presented includes measurements made over three consecutive years and a frozen zone is observed every year.~~
390 ~~According to the definition of permafrost (Harris et al., 1988) this can be treated as evidence of permafrost existence in high mountains (particularly Pirin Mountain) of Bulgaria~~the protection of glaciarret.

4 Conclusions

Detailed geophysical measurements of Snezhnika microglacier in Golyam Kazan, Pirin were conducted in 2018, 2019 and 2020 in order to estimate the thickness and internal structure of the ~~snow body and~~ glaciarret and the subsurface structure
395 beneath ~~and near it.~~ it. One of the main results from the study is the assessment of the ice thickness on a larger scale than it was made before. The mean thickness ~~is estimated from radargrams as~~ estimated from GPR profiles is about $4-6\,m$. In some places in the southern part of the ice body it reaches $8\,m$. ~~The estimated thickness shows~~ This results show partly agreement with the results from early borehole measurements and results obtained by Popov (1962) but the ~~depth~~ depths of 11 m (Gruenewald et al., 2008) ~~is~~ and 12 m (Onaca et al., 2022) are not detected. ~~Our GPR measurements~~ The reason for this can be that our GPR
400 profiles cover large but not the whole area of the microglacier~~and borehole measurement of the depth give information only in one point from the area. We assume that this is the reason of disagreement with the estimated from (Gruenewald et al., 2008) thickness~~. It is still not possible to estimate the changes in thickness of the microglacier through the years starting from 1962 due to insufficient data. However~~the obtained results for the thickness are~~, the thickness values estimated are a good base for ~~future monitoring of microglacier~~ monitoring the microglacier Snezhnika not only by size.

405 The ~~underlying layer is the glacial bed and consists of rock blocks of different sizes between which are filled with ice and water and voids. This layer is likely draining the melted glacial water, which is important for preservation of the snow patch. Microglacier drainage systems is fully situated beneath the surface as no or rare observed is surface water in Golyam Kazan cirque. The thickness of this layer varies from 1 to 4 m along the particular lines.~~

second significant finding is the indication of permafrost in Pirin Mountain. The data from GPR and ERT measurements

410 ~~were made also near Snezhnika microglacier. On the lowest situated GPR profiles from 2018 a zone with complex relief is distinguished. The zone is located~~ which complement each other allow us to distinguish a zone of ice-rich permafrost in the southern part of the ~~microglacier and reaches~~ microglaciers bed, between the head moraine ~~. ERT profiles show an anomaly at the same place with~~ and the ice. The zone has complex relief and lack of reflections in GPR profiles and very high resistivity, $\geqslant 60000 \ \Omega m$~~. Such values are~~, values typical for ice. ~~The high vales of resistivity and the lack of reflections on the GPR~~

415 ~~profiles give us a reason to conclude that the zone represents a frozen area.~~ ERT measurements were repeated in the next two years and the anomaly is observed all consecutive years. ~~Based on this we can also assume that we have evidences~~ This can be taken as an evidence of permafrost in Pirin ~~mountain~~Mountain. An important finding is also the obtained information on the hydrology of the microglaciers area and particularly the answer of the question: "Where the meltwater disappears?". This is also important for preservation of the snow and ice. We identified that the underlying layer is likely draining the melted glacial

420 water. Microglacier drainage systems is fully situated beneath the surface as surface water is rarely observed and in most cases it is only close to the glaciarret.

The frozen zone is situated in the southern part of the microglacier and exists beneath the ~~ice and without ice~~ snow (in 2018) and without snow cover as in late autumn of 2020, when the microglacier's size was smallest and no shading of the ice layer was possible. The area is closer to the Dzhamdzhiev ridge and is shaded from it for the most of the day in the summer. This

425 result suggest the importance of mountain ridge shading for the preservation of frozen subsurface areas in the Golyam Kazan cirque, Pirin Mountain ~~. The assumption is also supported by the fact that no frozen zone was obtained near the perennial snow patch in Banski Suhodol valley, where the snow field is in the middle of the valley and far less protected by shading from the surrounding mountain ridges~~but the role of the other factors should also be considered.

Data availability. Authors are happy to share data requested by email. Available data is: GPR data from Golyam Kazan (2018 and 2020);
430 ERT measurements in Golyam Kazan (2018, 2019 and 2020); GPS tracks of snowfields, photos and short meteorological records of the temperature, atmospheric pressure and humidity made in two points in Golyam Kazan. DTM with resolution 7.63 cm/pix was also constructed using UAV photogrammetry.

Author contributions. AK led ERT measurements and processed the data. CT led the GPR measurements and processed the data. GG led the projects and organized the field work. GG prepared the manuscript with contribution of all co-authors.

435   *Competing interests.*   The authors declare that they have no conflict of interest.

Acknowledgements. The work was supported by the Science Fund of Sofia University within the projects 80-10-126/21.04.2017, 80-10-217/26.04.2018 and 80-10-24/18.03.2020 and Science Fund of University of Mining and Geology within the project GPF-222/11.03.2019. All measurements were carried out with the participation of students from both universities. The authors thank the following students: Boriyana Chtirkova, Bojourka Georgieva, Daniel Ishlyamski, Dragomir Dragomirov, Yanko Ivanov, Spas Nikolov, Valentin Buchakchiev, Kalina Stoimenova and Angel Dimitrov. We thank also Vassil Gourev for sharing idea and knowledge of studying perennial snow patches in Bulgarian mountains. Measurements were performed with the permission of Pirin National Park administration.

References

Annan, P., J. Davis. Impulse radar sounding in permafrost. Radio Science, 11 (4), pp. 383-394, 1976

Annan, A. P., Practical Processing of GPR Data, Sensors and Software, Ontario, 1999.

Arcone, S.A. High Resolution of Glacial Ice Stratigraphy: A Ground-penetrating Radar Study of Pegasus Runway, McMurdo Station, Antarctica. Geophysics, 61, 1653–1663, 1996

Arcone, S.A., Lawson, D.E., and Delaney, A.J., Short-pulse radar wavelet recovery and resolution of dielectric contrasts within englacial and basal ice of Matanuska Glacier, Alaska. Journal of Glaciology, Vol. 41, pp. 68–86, 1995

Baker, G. S., T. E. Jordan, J. Pardy, An introduction to ground penetrating radar (GPR), Stratigraphic Analyses Using GPR, Geological Society of America DOI = 10.1130/SPE432, ISBN print: 9780813724324

Barry, R. & Gan, T.Y. The global cryosphere: past, present and future. Cambridge University Press, Cambridge, 2011

Berthling, I., Etzelmuller, B., Isaksen, K. and Sollid, J.L., Rock glaciers on Prins Karls Forland. II: GPR soundings and the development of internal structures. Permafrost and Periglacial Processes, 11 (4), 357-369, 2000

Blindow, N., The central part of the Filchner-Ronne Ice Shelf, Antarctica: Internal structures revealed by 40 MHz monopulse RES. Annals of Glaciology, Vol. 20, pp. 365–371, 1994

Boyadjiev, S. On the geology of Pirin Mountain. Annuaire de la Direction des Recherches Geologiques et Minieres 8, 89–125, 1959 (in Bulgarian)

Brown R, Petkova N., Snow Cover Variability in Bulgarian Mountainous Regions: 1931- 2000, International Journal of Climatology, 27, 1215-1229. DOI = 10.1002/joc.1468, 2007.

Damm, B., & Langer, M. Kartierung und Regionalisierung von Permafrostindikatoren im Rieserfernergebiet (Südtirol/Osttirol). Mitteilungen der Österreichischen Geographischen Gesellschaft, 148, 295-314, 2006

Dimovski, S., Stoyanov, N., Gyurov, C., Efficiency of electromotography for detailed geoelectrical mapping of nearsurface geological section, Bulaqua, 4, pp. 47-55, 2007

Dimovski, S., Stoyanov, N., Localization of suitable sites for the construction of monitoring wells in a small-scale rock complex, Annual of University of Mining and Geology "St. Ivan Rilski", 58(1), 140–145, 2015

Dobinski, W., Permafrost of the Carpathian and Balkan Mountains, eastern and southeastern Europe. Permafrost Periglac. Process., 16: 395-398, 2005. DOI = 10.1002/ppp.524

Dortman, N. B. Physical Properties of the Rocks and Mineral Resources. Handbook of the Geophysicist. Nedra, Moscow, 1984. (in Russian)

Emmert, A., Ch. Kneisel (2017) Internal structure of two alpine rock glaciers investigated by quasi-3-D electrical resistivity imaging. The Cryosphere, 11, 841–855, 2017

Etzelmüller, B., Frauenfelder, R., Factors Controlling The Distribution of Mountain Permafrost in The Northern Hemisphere and Their Influence on Sediment Transfer, Arctic, Antarctic, and Alpine Research, 41:1, 48-58, DOI = 10.1657/1523-0430-41.1, 2009

Evans, S. Dielectric properties of ice and snow - a review. Journal of Glaciology, Vol. 5, No. 42, p. 773-92, 1965

Fitzgerald, W.J., and Paren, J.G. The dielectric properties of Antarctic ice. Journal of Glaciology, Vol. 15, No. 73, p. 39-48, 1975

Fort M., Impact of climate change on mountain environment dynamics, Journal of Alpine Research, 103-2, DOI = 10.4000/rga.2877, 2015

Gadek, B., Grabiec, M. Glacial ice and permafrost distribution in the Medena Kotlina (Slovak Tatras): mapped with application of GPR and GST measurements. STUDIA GEOMORPHOLOGICA CARPATHO-BALCANICA, VOL. XLII, 5–22, 2008

Gachev, E., Climatic factors for the year-round dynamics of microglacier Snezhnika in Pirin, Scientific conference "Geographic aspects of planning and the use of the territory in the context of global changes", Extended Abstracts, 2016 (in Bulgarian)

480   Gachev, E., Holocene glaciation in the mountains of Bulgaria., Med. Geosc. Rev. 2, 103–117 DOI = 10.1007/s42990-020-00028-3 2020.

Gachev, E., Stoyanov, K., Gikov, A. Small glaciers on the Balkan Peninsula: State and changes in the last several years. Quaternary International 415. DOI = 10.1016/j.quaint.2015.10.042, 2016

Gachev, E. The Unknown Southernmost Glaciers of Europe. Glaciers evolution in a changing world. Zagreb. DOI = 10.5772/intechopen.68899, 2017a

485   Gachev, E. High mountain relief in marble in Pirin mountains, Bulgaria: Structure, specifics and evolution. Rev.Geomorfol., 19, 118-135, 2017b

Gachev, E., ~~Gikov, A., Zlatinova, C., Blagoev, B. Present state of Bulgarian glacierets. Landform Analysis, 11, 16-24, 2009~~ ~~Gachev, E. , Gikov, A. Description and first measurement of the snowfield in the Banski Suhodol circus. Problems of geography, 3-4.90-98, 2010~~ Mitkov, I., Small glaciers in Pirin (Bulgaria) and Durmitor (Montenegro) as glacio-karstic features. Similarities and differences in

490   their recent behaviour, Quaternary International, Vol. 504, 153-170, ISSN 1040-6182, DOI = 10.1016/j.quaint.2018.03.032, 2019

Georgieva, G., Kisyov, A., Tzankov, C., Chtirkova, B., Gourev, V., Ivanov, Y., Evaluation of geophysical methods for studying snowfields in Pirin Mountain, Bulgaria Extended abstract from 10th Congress of Balkan Geophysical Society, BGS 2019. DOI = 10.3997/2214-4609.201902662, 2019

Glazirin, G. E., Kodama, Y., Ohata, T., Stability of drifting snow-type perennial snow patches Bull. of Glaciol. Research, vil. 21, 1-5, 2004

495   Gruber S., Haeberli W. Mountain Permafrost. In: Margesin R. (eds) Permafrost Soils. Soil Biology, vol 16. Springer, Berlin, Heidelberg. DOI = 10.1007/978-3-540-69371-0_3, 2009

~~Grünewald K., Weber C., Scheithauer J. & Haubold, E., Mikrogletscher als Klimaindikatoren und Umweltarchive in sudosteuropaischen Hochgebirgen? - Untersuchung des Vichrengletschers im Piringebirge (Bulgarien). Zschr. Gletscherkunde und Glazialgeologie, 99–114, 2006~~

500   Grunewald, K., Scheithauer, J. Klima- und Landschaftgeschichte Sudosteuropas. Rekonstruktion anhand von Geoarchiven im Piringebirge (Bulgarien). Rhombos Verlag, Berlin,178 pp, 2008

Gruenewald, K., Scheithauer, J., Gikov, A., Microglaciers in the Pirin Mountains, Problems of Geography, 1–2, 1–16, 2008 (in Bulgarian).

Grunewald, K., & Scheithauer, J. Europe's southernmost glaciers: Response and adaptation to climate change. Journal of Glaciology, 56(195), 129-142. DOI = 10.3189/002214310791190947, 2010

505   Grunewald, K., & Scheithauer, J. Europe's southernmost glaciers: response and adaptation to climate change. Journal of glaciology, 56(195), 129-142, 2010

Guodong, C. and Dramis F., Distribution of mountain permafrost and climate. Permafrost and Periglacial Process., 3, 83-91, 1992

Haberkorn A, Kenner R, Noetzli J and Phillips M., Changes in Ground Temperature and Dynamics in Mountain Permafrost in the Swiss Alps. Front. Earth Sci. 9:626686. DOI = 10.3389/feart.2021.626686, 2021

510   Harris, S. A.; French, H. M.; Heginbottom, J. A.; Johnston, G. H.; Ladanyi, B.; Sego, D. C.; van Everdingen, R. O., Glossary of permafrost and related ground-ice terms, Technical Memorandum (National Research Council of Canada. Associate Committee on Geotechnical Research), no. ACGR-TM-142,159 p. DOI = 10.4224/20386561, 1988

Hughes, P.D. Little Ice Age glaciers in the Mediterranean mountains. Mediterranee, 122, 63-79, 2014

Hughes, P.D.. Little Ice Age glaciers and climate in the Mediterranean mountains: a new analysis., Cuadernos de Investigación Geográfica,

515   44.1, 15-45, 2018

Hauck, C., Geophysical methods for detecting permafrost in high mountains, Versuchsanstalt ~~fUr~~ für Wasserbau Hydrologie und Glaziologie der Eidgenossischen. Technischen Hochschule Zurich, ISSN 0374-0056, 2001

Hauck, C.: New Concepts in Geophysical Surveying and Data Interpretation for Permafrost Terrain, Permafrost Periglac., 24, 131– 137, doi:10.1002/ppp.1774, 2013.

520   Hausmann, H., Krainer, K., Brück, E., and Ullrich, C.: Internal structure, ice content and dynamics of Ölgrube and Kaiserberg rock glaciers (Ötztal Alps, Austria) determined from geophysical surveys, Austrian Journal of Earth Sciences, 105, 12–31, 2012.

Haeberli, W., Untersuchungen zur Verbreitung von Permafrost zwischen Flüelapass und Piz Grialetsch (Graubünden). Mitteilung der Versuchsanstalt für Wasserbau, Hydrologie und Glaziologie, 1975, 18, 7-128.

Hilbich, C.,Marescot, C. L. Hauck, C., Loke, M. H., Mäusbacher, R., Applicability of Electrical Resistivity Tomography Monitoring to
525   Coarse Blocky and Ice-rich Permafrost Landforms. Permafrost and Periglacial Processes 20(3): 269-284, 2009

Hinkel, K.M., J.A. Doolittle, J.G. Bockheim, F.E. Nelson, R. Paetzold, J.M. Kimble, R. Travis. Detection of subsurface permafrost features with ground-penetrating radar, Barrow Alaska Permafrost and Periglacial Processes, 12, pp. 179-190, 2001

Hoekstra, P. & McNeill, D. Electromagnetic probing of permafrost. In North American Contribution, Second International Conference on Permafrost, Yakutsk, USSR (pp. 517–526). Washington DC: National Academy of Sciences, 1973

530   Hoekstra, P. & Delaney, A. Dielectric properties of soils at UHF and microwave frequencies. Journal of Geophysical Research Journal of Geophysical Research, 79(11), 1699–1708, 1974

Ikeda, A.: Combination of conventional geophysical methods for sounding the composition of rock glaciers in the Swiss Alps, Permafrost Periglac., 17, 35–48, doi:10.1002/ppp.550, 2006

Ingeman-Nielsen, T., Geophysical techniques applied to permafrost investigations in Greenland. Ph.D. Thesis BYG DTU R-123 Arctic
535   Technology Centre Department of Civil Engineering Technical University of Denmark, ISSN 1602-2917, 2005

Jol, Harry M. (Editor), Ground Penetrating Radar Theory and Applications (1st Edition). Elsevier, p. 544. ISBN 9780444533487 7, 2009

Jørgensen, A. S., F. Andreasen. Mapping of permafrost surface using ground-penetrating radar at Kangerlussuaq Airport, western Greenland. Cold Regions Science and Technology, 48, 1, 64-72, 2007

Kawashima, K., Yamada, T., & Wakahama, G. Investigations of internal structure and transformational processes from firn to ice in a
540   perennial snow patch. Annals of Glaciology, 18, 117-122. DOI = 10.3189/S0260305500011368, 1993

King, M. S. The influence of clay-sized particles on seismic velocity for Canadian Arctic Permafrost. Canadian Journal of Earth Sciences, 21(1), 19–24, 1984

King, M. S., Zimmerman, R. W., & Corwin, R. F. Seismic and electrical properties of unconsolidated permafrost. Geophysical Prospecting, 36(4), 349–364, 1988

545   Kisyov,A., Tzankov, Ch., Chtirkova, B., Georgieva, G., Ivanov, Y., Georgieva, B., Ishlyamski, D., Gourev, V., Nikolov, S., Study of perennial snow patches in Bulgaria, Proceedings of IX National Geophysical Conference, 2018, Sofia (In Bulgarian)

Kneisel, C. & Kääb, A.: Mountain permafrost dynamics within a recently exposed glacier forefield inferred by a combined geomorphological, geophysical and photogrammetrical approach, Earth Surf. Proc. Land., 32, 1797–1810, doi:10.1002/esp.1488, 2007

Kneisel, C., Hauck, C., Fortier, R., and Moorman, B.: Advances in geophysical methods for permafrost investigations, Permafrost and
550   Periglacial Process, 19, 157–178, DOI = 10.1002/ppp.616, 2008

Lawson, D.E., Strasser, J.C., Evenson, E.B., Alley, R.B., Larson, G.J. and Arcone, S.A., Glaciohydraulic supercooling: A freeze-on mechanism to create stratified, debris-rich basal ice: I. Field evidence. Journal of Glaciology, Vol. 44, pp. 547-562, 1998

Loke, M. and Barker, R., Rapid leastsquares inversion of apparent resistivity pseudosections by a quasi Newton method. Geophysical Prospecting, 44: 131-152. DOI = 10.1111/j.1365-2478.1996.tb00142.x, 1996

555   Mares, S. and Tvrdý, M., Introduction to Applied Geophysics. Springer Netherlands; pp. 581; ISBN 978-90-277-1424-4, 1984

Maurer, H. & Hauck, C.: Geophysical imaging of alpine rock glaciers, J. Glaciol., 53, 110–120, DOI = 10.3189/172756507781833893, 2007.

Milner, A.M., Brown, L.E. & Hannah, D.M. Hydroe-cological response of river systems to shrinking glaciers. Hydrological Processes,23,62–77, 2009

Navarro, F.; Eisen, O. Ground-penetrating radar in glaciological applications. Remote Sens. Glaciers, 195–229, 2009

560   Olhoeft, G.R., Electrical properties of permafrost. 3nl International Confenmce on Pennafmst, Edmonton. Pmceedings, 1, 127- 131, 1978

Onaca, A., A. C. Ardelean, P. Urdea, F. Ardelean, F. Sîrbu. Detection of mountain permafrost by combining conventional geophysical methods and thermal monitoring in the Retezat Mountains, Romania. Cold Regions Science and Technology, 119, 111-123, 2015

Onaca, A., F. Ardelean, A. Ardelean, B. Magori, F. Sirbu, M. Voiculescu, E. Gachev, Assessment of permafrost conditions in the highest mountains of the Balkan Peninsula, CATENA, 185, 104-288, 2020 ISSN 0341-8162, DOI = 10.1016/j.catena.2019.104288

565   Onaca, A., Gachev, E., Ardelean, F., Ardelean, A., Persoiu, A., Hegyi, A., Small is strong: Post-LIA resilience of Europe's Southernmost glaciers assessed by geophysical methods, CATENA, Vol. 213, 106143, ISSN 0341-8162, DOI = 10.1016/j.catena.2022.106143, 2022

Pipan, M., Baradello L., Forte E., Prizzon A. Finetti I. 2-D and 3-D processing and interpretation of multi-fold ground penetrating radar data: a case history from an archaeological site J. appl. Geophys., 41, 2-3, 271-292, 1999

Pipan, M., Baradello, L., Forte, E., Prizzon, A. , Polarization and kinematic effects in azimuthal investigations of linear structures with
570   Ground Penetrating Radar, Proceedings of the Symposium on the Application of Geophysics to Engineering and Environmental Problems EEGS, 433-442, 2000

Popov, V., Morphology of the Cirque Golemia Kazan – Pirin Mountains, Announcements of the Institute of Geography, vol. 6, pp. 86-99, 1962 (in Bulgarian)

Popov, V., Observations on the Glacieret in the Cirque Golemia Kazan, the Pirin Mountains, Announcements of the Institute of Geography,
575   Bulgarian Academy of Sciences, vol. 7, pp. 198-207, 1964 (in Bulgarian)

Rolshoven, M., Alpines Permafrostmilieu in der Lasörlinggruppe/ Nördliche Deferegger Alpen (Osttirol)). Polarforschung,1982, 52, 55-64, DOI = 10013/epic.29521

Scott W, Sellmann P, Hunter J. Geophysics in the study of permafrost. In Geotechnical and Environmental Geophysics, Ward S (ed). Society of Exploration Geophysics: Tulsa; 355–384, 1990

580   Supper, R., D. Ottowitz, B. Jochum, A. Romer1, S. Pfeiler, S. Kauer, M. Keuschnig, A. Ita. Geoelectrical monitoring of frozen ground and permafrost in alpine areas: field studies and considerations towards an improved measuring technology. Near Surface Geophysics, 12, 93-115, 2014

Telford, W.M., Geldart, L.P. and Sheriff, R.E., Applied geophysics. 2nd edition, Cambridge University Press, 1990

van der Kruk, J., Wapenaar, C.P.A., Fokkema, J.T., Van den Berg, P.M. Three-dimensional imaging of multicomponent ground-penetrating
585   radar data Geophysics, 68, 4, 1241-1254, DOI = 10.1190/1.1598116, 2003

Watanabe T. Studies of snow accumulation and ablation on perennial snow patches in the mountains of Japan. Progress in Physical Geography: Earth and Environment. 12(4):560-581. DOI = 10.1177/030913338801200404, 1988

Washburn, A. L. Geocryology - A survey of periglacial processes and environments. University of Washington, 1979

Williams, K. E., McKay, C. P., Toon, O. B., Jennings, K. S., Mass balance of two perennial snowfields: Niwot Ridge, Colorado, and the
590   Ulaan Taiga, Mongolia, Arctic, Antarctic, and Alpine Research, vol. 54,No. 1, p 41-61, DOI = 10.1080/15230430.2022.2027591, 2022

Yakupov, V.S., Electrical conductyvity of frozen roks. Permafrost: Second International Conference, July 13-28, National academy of sciences, Washington, D.C., 1973

Zemp, M., Glaciers and Climate Change - Spatio-temporal Analysis of Glacier Fluctuations in the European Alps after 1850, Dissertation, Zürich, 2006

595   Zhao, W., Tian, G., Forte, E., Pipan, M., Wang, Y., Li, X., Shi, Z., Liu, H. Advances in GPR data acquisition and analysis for archaeology Geophys. J. Int., 202, 1, 62-71, 2015

Zhao, W., Forte, E. Colucci, R.R, Pipan, M., High-resolution glacier imaging and characterization by means of GPR attribute analysis, Geophysical Journal International, 206, 2, 1366–1374, DOI = 10.1093/gji/ggw208, 2016